Unhydrated Cr(V) Peroxychromates M_3CrO_8 (M = Na, K, Rb): Low-Dimensional Antiferromagnets Exhibiting Large Specific Heats at mK to 5 K Temperatures

Brant Cage and Nar S. Dalal*

Department of Chemistry and National High Magnetic Field Laboratory, Florida State University, Tallahassee Florida, 32306-4390

Received August 11, 2000. Revised Manuscript Received December 15, 2000

The alkali-metal Cr(V) peroxychromates with the general formula M_3CrO_8 (M = Na, K, Rb, and combinations thereof) and the $3d^1$ ground state have been characterized by X-ray diffraction, variable frequency and variable temperature EPR, magnetic susceptibility, and thermodynamic techniques. K_3CrO_8 and Rb_3CrO_8 are isomorphous, with space groups as $I\bar{4}2m$, whereas Na_3CrO_8 and K_2NaCrO_8 exhibit the orthorhombic space groups *Cmc*2 and *Pbcm*, respectively. Lattice parameters are presented for all of these compounds and are shown to depend sensitively on the cation. EPR measurements reveal that while the electronic ground state of Na_3CrO_8, K_3CrO_8, and Rb_3CrO_8 is $3d_{x^2-y^2}$, that of the mixed salts, such as K_2NaCrO_8 and Rb_2NaCrO_8, is $3d_{z^2}$; the origin of this switch is not yet clear. Specific heat measurements showed that K_3CrO_8 undergoes an antiferromagnetic ordering transition at $T_N = 0.38$ K and displays a broad peak around 0.8 K, which can be interpreted in terms of a Bonner−Fisher model. Rb_3CrO_8 behaves similarly, with a broad peak at 0.52 K. Na_3CrO_8 exhibits a λ-like antiferromagnetic transition at 2.35 K, with K_2NaCrO_8 behaving similarly, with T_N lower than 1.8 K. The exchange constants and the transition temperatures depend sensitively on the cation. These compounds all are found to exhibit large specific heats throughout the mK to 5 K temperature range, and the possibility exists of tuning the thermodynamic properties via dilution with compatible diamagnetic lattices such as M_3NbO_8. Their specific heat data indicate that they could find applications as tunable heat sinks and magnetic refrigerants in the mK to 5 K range.

I. Introduction

This paper reports on an improved crystal growth procedure, X-ray structural analysis, thermomagnetic and spectroscopic measurements, and the finding of some interesting new electronic and magnetic properties of the alkali-metal peroxychromates, M_3CrO_8 (M = Na, K, Rb, and combinations thereof). The Cr ion here is in its rather unusual, pentavalent, ($3d^1$) oxidation state. The motivations for this undertaking were manifold. First, while the M_3CrO_8 salts were first reported[1] in 1905, not much is known about their electronic structure and bulk thermodynamic properties, perhaps because they are thought to be unstable and hard to grow as large crystals.[2] Second, they are model compounds from theoretical aspects since there are few such simple (i.e., nd^1 $S = {}^1/_2$, $I = 0$) Kramers' ions available for theoretical and experimental work. Chief among those in use are Ti(III) and V(IV). Ti(III) compounds are generally air-sensitive, complicating experimental work, and they are difficult to understand theoretically. The presence of low-lying excited states[3] makes the spin−lattice relaxation time of Ti(III) compounds generally very short, so their electron paramagnetic resonance (EPR) spectra are usually only obtainable at helium temperatures. For example, Ti(III) diluted into cesium aluminum alum has been shown[3] to exhibit a dynamic Jahn−Teller effect, large spin−orbit coupling, and a trigonal distortion giving rise to a zero-field splitting and multiple EPR lines for single crystals. V(IV) exists mainly as the VO^{2+} ion and the major isotope (^{51}V, 99.7% natural abundance) has a large nuclear spin of $^7/_2$. This results in hyperfine complications and up to eight EPR lines in the absence of exchange narrowing.[4] In contrast, the $S = {}^1/_2$, $I = 0$ electronic structure of the main $^{50,52,54}Cr$ isotopes (90.5% natural abundance) renders the M_3CrO_8 compounds[2] as being among the simplest of magnetic lattices. The general chemical structure of the CrO_8^{3-} ion is shown in Figure 1. At room temperature and up to 95 GHz, single-crystal EPR spectra of these compounds are expected to exhibit a single exchange-narrowed EPR line,[5] and the magnetic susceptibility to follow the Curie−Weiss behavior down to liquid helium temperatures, as was reported[6] earlier for K_3CrO_8.

* To whom correspondence should be addressed. E-mail: dalal@chem.fsu.edu.

(1) Riesenfeld, E. H. *Chem. Ber.* **1905**, *38*, 4068.
(2) For a recent review, see Dickman, M. H.; Pope, M. T. *Chem. Rev.* **1994**, *94*, 569−84.
(3) Shing, Y. H.; Walsh, D. *Phys. Rev. Lett.* **1974**, *33*, 1067−69.
(4) For a review of oxovanadium (IV) complexes, see Syamal, A. *Coord. Chem. Rev.* **1975**, *16*, 309−39.
(5) Cage, B.; Cevc, P.; Blinc, R.; Brunel, L.-C.; Dalal, N. S. *J. Magn. Reson.* **1998**, *135*, 178−84.
(6) Dalal, N. S.; Millar, J. M.; Jagadeesh, M. S.; Seehra, M. S. *J. Chem. Phys.* **1981**, *74*, 1916−22.

10.1021/cm000643d CCC: $20.00
Published on Web 02/08/2001

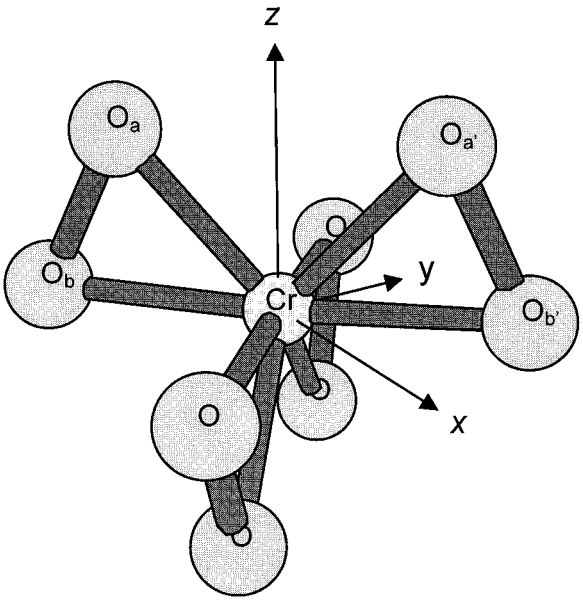

Figure 1. Schematic of the structure of the CrO_8^{3-} anion.

Thus far, the most detailed and systematic theoretical[7] as well as experimental[6,8] work on the electronic and magnetic properties of $3d^1$ systems has been reported only on K_3CrO_8. While these studies have yielded significant insights into the overall electronic structure and specifically the metal−dioxygen bonding here, there are discrepancies regarding the finer details, as for example, on whether the unpaired electron is localized mainly on the peroxo ligands[7b] or on the Cr ion.[7a,d] The current view, which is also in agreement with some earlier EPR studies,[6,8] is that the unpaired spin density is mainly on the metal,[7c] but with a significant back-donation from the oxygen ligands. On this basis, one expects the presence of electron−electron-superexchange interactions with neighboring Cr ions, and thus some unusual magnetic properties and possibly even phase transitions in these systems. Thus far, however, there has been no report of any structural or magnetic phase transitions in these materials, and a search for this possibility was the main trigger for the present undertaking.

II. Experimental Section

Synthesis and Crystal Growth. The synthesis of the peroxychromates was accomplished by modification of the method of Riesenfeld.[1] In general, the synthesis involves the reduction of Cr(VI) by H_2O_2 in the appropriate base or mixture of bases at temperatures of 5 °C. A significant finding was that good quality crystals are obtainable only by crystallization around room temperature. Earlier reports[1,6] had mentioned lower temperatures around −15 °C, which we found suitable for the synthesis, but not for good quality crystals, *which were crucial for this study*.

Specifically, 20 g of CrO_3 was dissolved in 200−300 mL of an aqueous MOH (M= Na, K, Rb, and combinations thereof) 25% solution (by weight, pH = 12−14) and cooled in an ice bath to ∼5 °C. Then, 40−60 mL of cold H_2O_2 was added dropwise without stirring over the course of 3 h. The black red solution was placed in the refrigerator at 5 °C for 3−5 days. Growth by slow evaporation produced dark red parallelepiped-shaped crystals of typical $1 \times 1 \times 3$ mm^3 size. A preliminary account has been published earlier.[9]

Crystal Structure. The crystal structures were obtained[10] by X-ray diffraction on Na_3CrO_8, K_3CrO_8, K_2NaCrO_8, and Rb_3CrO_8. Table 1 provides a summary of the observed crystal parameters. Atomic coordinates are available from the authors[10] and will be deposited with the Cambridge database. The relations of the crystal morphology to the crystal axes for all samples are given in Appendix A.

Specific Heat Measurements. Specific heat measurements over a range from 0.15 to 3 K were made on K_3CrO_8 at Carnegie-Mellon University using a homemade adiabatic calorimeter, as described elsewhere.[9]

Specific heat measurements between 1.8 and 10 K and 0−9 T were made using a Quantum Design Physical Properties Measurement System (QD PPMS) employing a time constant[11] method at Florida State University. The platform was calibrated by use of a copper standard.[12] The samples consisted of multiple crystals of Na_3CrO_8, eight crystals (aligned for the isotherm experiment) of K_2NaCrO_8, and single crystals of K_3CrO_8 and Rb_3CrO_8. The typical sample mass was 2−3 mg.

Magnetic Measurements. dc magnetic susceptibility (χ) measurements were made on aligned multiple crystals of K_3CrO_8 (sample size ∼3−4 mg), an aligned single crystal of Rb_3CrO_8 (sample mass 22.76 mg), and multicrystalline samples of Na_3CrO_8 (∼8 mg) and K_2NaCrO_8 using a Quantum Design SQUID magnetometer at a magnetic field of 3000 Gauss (G) (10 000 G = 1 Tesla (T)). For all samples χ was observed to be independent of the fields at all temperatures used in this investigation. ac susceptibility data for K_3CrO_8 and Rb_3CrO_8 were obtained using a homemade ac susceptometer (static field ∼100 G) and a dilution refrigerator in the 300 mK to 1.2 K range, as described elsewhere.[9]

EPR Measurements. *X*-band (∼9.5 GHz) EPR measurements were made using a Varian E-12 spectrometer. The microwave frequency was measured with a Hewlett-Packard (model 5340A) digital frequency counter. *W*-band (∼95 GHz) data were obtained using a homemade microwave bridge and a Quantum Design 9 T PPMS magnet. The frequency was measured with an EIP model 578B Source Locking Microwave Counter. The magnetic field was calibrated using DPPH and 0.5% K_3CrO_8 diluted into a diamagnetic K_3NbO_8 matrix, as discussed elsewhere.[13] All reported values of the **g** tensors were obtained at the *W* band and all measurements were made at room temperature.

III. Results and Discussion

III.A. Evidence for Phase Transitions. A major goal of this investigation was to search for antiferromagnetic or other types of phase transitions in the M_3CrO_8 ($3d^1$) lattices. For this purpose, we carried out heat capacity, magnetization, and EPR spectroscopic measurements. Since K_3CrO_8 is well-studied and is a prototype lattice in this system, we begin with the measurements for this lattice. Earlier studies[6] involving

(7) (a) Swalen, J. D.; Ibers, J. A. *J. Chem. Phys.* **1962**, *37*, 17−20. (b) Fischer, J.; Veillard, A.; Weiss, R. *Theor. Chim. Acta* **1972**, 1426. (c) Roch, M.; Weber, J.; Williams, A. F. *Inorg. Chem.* **1984**, *23*, 4571−80. (d) Weber, J.; Roch, M.; Williams, A. F. *Chem. Phys. Lett.* **1986**, *123*, 246−53.

(8) (a) McGarvey, B. R. *J. Chem. Phys.* **1962**, *37*, 2001−04. (b) Dalal, N. S.; Suryan, M. M.; Seehra, M. S. *Anal. Chem.* **1981**, *53*, 938−40.

(9) Cage, B.; Singh, K.; Friedberg, S.; Shimuzu, S.; Moodera, J. S.; Lawless, W. N.; Dalal, N. S. *Solid State Commun.* **2000**, *113*, 93−97.

(10) For Na_3CrO_8, Abboud, K. A., University of Florida, unpublished results. For K_2NaCrO_8, Craven, B., University of Pittsburgh, and Abboud, K. A., University of Florida, unpublished results. For Rb_3CrO_8, Cherry, W. R., Louisiana State University, unpublished results. For K_3CrO_8, Stomberg, R.; Brosset C. *Acta Chem. Scand.* **1960**, *14*, 441−52, and Wood, R. M.; Abboud, K. A.; Palenik, R. C.; Palenik, G. J. *Inorg. Chem.* **2000,** *39*(10), 2065−68.

(11) For a review of low-temperature calorimetry, see Stewart, G. R. *Rev. Sci. Instrum.* **1983,** *54*, 1−11.

(12) Leyarovski, E. I.; Leyarovska, L. N.; Popov, C.; Popov, O. *Cryogenics* **1987**, *28*, 321−35.

(13) Cage, B.; Weekley, A.; Brunel, L.-C.; Dalal, N. S. *Anal. Chem.* **1999**, *71*, 1951−7.

Table 1. Crystal Parameters of the Peroxychromates[10] (Å)

	Na_3CrO_8	K_3CrO_8	Rb_3CrO_8	K_2NaCrO_8
crystal class	orthorhombic	tetragonal	tetragonal	orthorhombic
space group	*Cmc*2(1)	$I\bar{4}2m$	$I\bar{4}2m$	Pbcm
a	8.6166	6.6940	6.9759	8.6031
b	8.1186	6.6940	6.9759	7.9792
c	7.9198	7.5736	7.8176	9.2520
nearest neighbor (NN)	5.53	6.06	6.29	5.84
NN superexchange	6.36	6.76	6.96	6.70
second NN	5.81	6.69	6.98	5.98
second NN superexchange	6.91	7.85	8.16	7.16

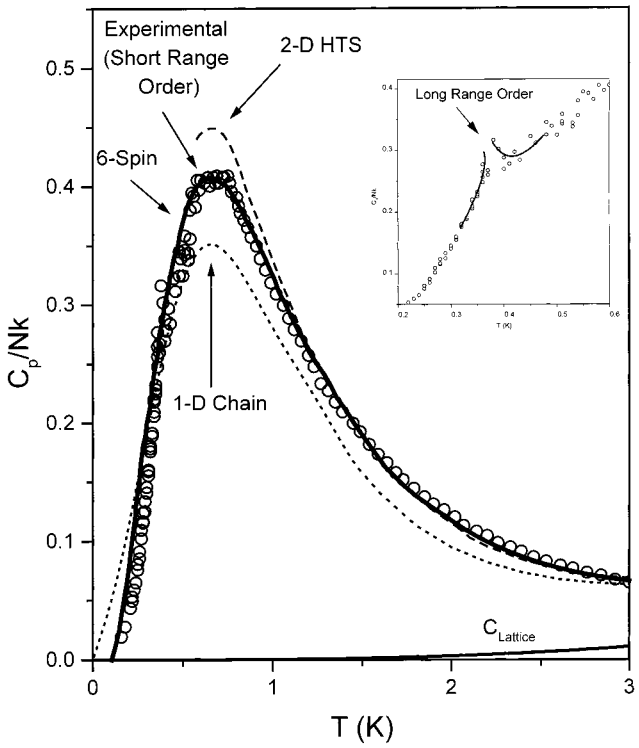

Figure 2. Specific heat of K_3CrO_8. Open circles (○) are the measured data points. The continuous and dotted lines are the Bonner−Fisher $1D_{N=6}$ and $1D_{N=\infty}$ fits, while the dashed line is the 2D HTS. Solid line at the bottom is the estimated lattice term. Inset provides a magnification of the 0.2−0.6 K region. The drawn line is a guide for the eyes.

magnetic susceptibility from 343 to 1.4 K had concluded that K_3CrO_8 exhibits no magnetic transition over this range. Therefore, measurements below 1.4 K were deemed necessary.

III.A.a. Heat Capacity Measurements on K_3CrO_8. The specific heat of K_3CrO_8 as a function of temperature from 0.20 to 3.00 K is presented as open circles in Figure 2. This broad maximum is characteristic of low-dimensional cooperative phenomena and may be examined in the context of the isotropic ($\alpha = \gamma = 1$) Heisenberg spin interaction Hamiltonian:

$$H = -2J\sum_{i=1}^{N}\alpha(S_i^z S_{i+1}^z) + \gamma(S_i^x S_{i+1}^x + S_i^y S_{i+1}^y) \quad (1)$$

Bonner and Fisher[14] computed the specific heat and susceptibility of short chains (or closed rings) for $N = 1$ to $N = 11$ (where at higher values of N the behavior is similar) and extrapolated to $N = \infty$. It was found that, for the K_3CrO_8 data, the best fit[15] was for antiferromagnetic coupling with $N = 6$, which is shown as the solid line in Figure 2. This fit is characterized by $kT_{max}/|J| = 0.87$ and $C_{max}/Nk = 0.40$, in agreement with experimental data. The solid curve yielded $J/k = -0.76$ K, which will be compared to that obtained from χ in section III.A.c. For comparison, the fit for $N = \infty$ is given as the dotted line,[14] as is the high-temperature series expansion (HTS) for a two-dimensional (2D) quadratic lattice[16−18] (dashed line); the corresponding exchange energies are provided in Table 3. Further discussion and a comparison of these models as related to the crystal structure are provided in section III.B.

The inset to Figure 2 shows an enlarged view over the temperature region of 0.2−0.6 K. The small sharp peak at 0.38 K (the drawn line is a guide for the eye) is postulated to be resulting from long-range antiferromagnetic three-dimensional (3D) ordering. This peak is thus representative of the Neel temperature because a sharp peak in the specific heat is quite characteristic of long-range order, that is, a phase transition. Evidence of the magnetic origin of these two peaks is presented in the magnetic susceptibility section. Additionally, we employed an analytic method comparing the observed entropy with the theoretically expected magnetic contribution, as discussed below.

III.A.b. Nature of the Entropy Change for K_3CrO_8. The experimental entropy at constant field of the system is determined using the relation[19]

$$\Delta S = \int_{T_1}^{T_2} C_H \frac{dT}{T} \quad (2)$$

Therefore, integration of C/T vs T yields the total entropy. This was found to be 5.9 ± 0.2 J/(mol·K) over the temperature range of 0.2−3 K. The lattice contribution[15] to the entropy over this temperature range for K_3CrO_8 is estimated to be ∼0.015 J/(mol·K).

(14) Bonner, J. C.; Fisher, M. E. *Phys. Rev.* **1964**, *135*, 3A, 640−58.

(15) For an insulating paramagnet the main contributions to the heat capacity in this region are composed of the lattice and magnetic terms such that $C_{total} = C_{lattice} + C_{magnetic}$. In this low-temperature region $C_{lattice}$ may be approximated by the Debye cube law such that $C_{lattice} = \alpha T^3$. The best fit was obtained using $\alpha = 0.0017$, 0.0066, and 0.0072 J/(mol· K^4) for $N = 6$, ∞ chains, and two dimensions, respectively.

(16) Algra, H. A.; De Jongh, L. J.; Carlin, R. L. *Physica B+C*, **1978**, *93B*, 24−34; **1978**, *95B*, 224.

(17) See, for example, Navarro, R. *Magnetic Properties of Layered Transition Metals*; de Jongh, L. J., Ed.; Kluwer Academic Pub.: Dordrecht, The Netherlands, 1990; pp 105−190.

(18) The $N = \infty$ and 2D specific heat fits are characterized by $kT_{max}/|J| = 0.962$ and ∼1.3, respectively.

(19) Carlin, R. L.; Van Duyneveldt, A. J. *Magnetic Properties of Transition Metal Compounds*; Springer-Verlag: New York, 1977; pp 25, 56−62, 123. Carlin, R. L. *Magnetochemistry*; Springer-Verlag: New York, 1986; p 178.

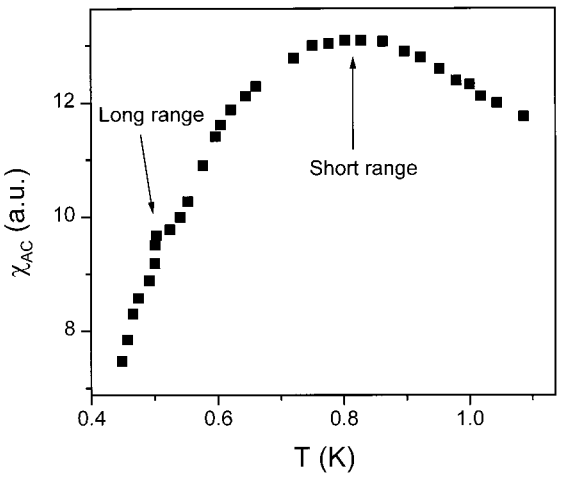

Figure 3. Temperature dependence of the *ac* susceptibility, χ_{ac} (arbitrary units), of K_3CrO_8 in the ^{3}He temperature range. Clearly visible are the broad peak around 0.82 K and a sharp peak at 0.52 K, as highlighted by arrows.

The maximum theoretical magnetic entropy is given by

$$S = R \ln(2J_{am} + 1) \quad (3)$$

where J_{am} is the total angular momentum $J_{am} = (L + S)$ (L the orbital and S the spin angular momentum). Assuming that the orbital contribution is quenched, then $L = 0$; therefore, $J = S = {}^1/_2$. Using eq 3, the theoretical magnetic contribution to the total entropy is 5.76 J/(mol·K). Therefore, this analytic approach indicates that the observed entropy over the temperature range of 0.2−3 K is within experimental error of that expected for a $S = 1/2$ system, with the low-dimensional interactions being the dominating term. This implies that a majority of the magnetic entropy is involved in short-range spin ordering; thus, the transition to long-range order requires a very small entropic change, in agreement with the low magnitude of the peak at the Neel temperature of 0.38 K.

III.A.c. *ac* Susceptibility Data and the Phase Transition of K_3CrO_8. To further understand the nature of the observed heat capacity anomalies, we measured magnetic susceptibility over the same temperature range. Measurements of the *ac* susceptibility (in arbitrary units) of K_3CrO_8 powder, shown in Figure 3, yielded a broad peak at 0.82 K and a small but clear bump at 0.52 K. Qualitatively, Figure 3 is in general agreement with the Fisher relationship[20] of the temperature variation of the specific heat (Figure 2) to the susceptibility of an antiferromagnet. According to this relationship, any anomaly in the magnetic heat capacity is associated with a similar anomaly in $\partial(\chi_{\parallel}T)/\partial T$, implying that the maximum in χ is somewhat above the actual ordering temperature observed in C_p, as is the case here. Therefore, the peaks in C_p (Figure 2) are of a magnetic origin.

Quantitatively, one can compare the temperature of the observed maximum in the magnetic moment to that expected for a six-spin Bonner−Fisher linear chain system, which is[14]

$$kT_{max}/|J| \cong 1.38 \quad (4)$$

This relationship yields a value of $J/k = -0.60$, compared to $J/k = -0.76$ K as determined from heat capacity. We consider this as a close agreement between the heat capacity and the magnetic moment of K_3CrO_8 to the six-spin linear chain model. We can thus assign the broad maxima in Figures 2 and 3 to short-range ordering through magnetic exchange interactions and the sharp small spikes to long-range antiferromagnetic ordering.

III.B. Low-Dimensional Behavior as Related to the Crystal Structure of K_3CrO_8. The observed low-dimensional behavior of K_3CrO_8 can be qualitatively understood in terms of its crystal structure. As first reported by Stomberg,[10] K_3CrO_8 crystallizes in the tetragonal system (see Table 1). Figure 4 depicts the K_3CrO_8 lattice projected down the *b* axis. It can be seen herein that the Cr(V) ions form a two-dimensional square lattice in the *ab* plane, whereas they are alternated by a K ion along the longer, unique *c* axis. However, the absolute fit of a square lattice (Figure 2, dashed line) to the heat capacity is somewhat unsatisfactory, although there is reasonable agreement of exchange energies between C_p and χ (Table 3). Possibly, a lattice distortion may occur at low temperatures, as is the case for the copper-pyridine-*N*-oxide salts[16,21] that would tend to favor exchange along either the *a* or the *b* axis. However, like the two-dimensional model, the fit to heat capacity for an infinite chain (Figure 2, dotted line) is unsatisfactory, even though the exchange energies are in agreement. Interestingly, the fit for $N = 6$ (Figure 2, solid line) is quite good, suggesting a collection of short chains or rings; unfortunately, there is no good model available that might explain how these short chains may arise.

These questions may be answered by local measurements such as EPR at low temperatures. The orientation dependence of the line width to the Zeeman field[22,23] and the frequency dependence at the magic angle[24,25] can provide valuable information as to the spin exchange dimensionality. EPR may also reveal the existence of a possible lattice distortion, as was the case for the copper-pyridine-*N*-oxides,[26] and experiments are currently underway. Neutron diffraction and crystal structures at these low temperatures would also prove quite fruitful.

III.C.a. Magnetic Susceptibility of Rb_3CrO_8. To examine the generality of the K_3CrO_8 data, we investigated Rb_3CrO_8, which is isostructural[10] (see Table 1) to K_3CrO_8. Figure 5 shows a plot of the dc magnetic susceptibility vs temperature from 1.8 to 20 K of a single crystal of Rb_3CrO_8 oriented with the *c* axis parallel and

(20) Fisher, M. E. *Proc. R. Soc. (London)* **1960**, *A254*, 66.
(21) Carlin, R. L.; de Jongh, L. J. *Chem. Rev.* **1986,** *86*, 659−80.
(22) Bencini, A.; Gatteschi, D. *EPR of Exchange Coupled Systems*; Springer-Verlag: New York, 1990; p 135.
(23) Cage, B.; Geyer, W.; Abboud, K. A.; Dalal, N. S. *Chem. Mater.* **2001**, *13*, 871−879.
(24) Benner, H.; Boucher, J. P. R. *Magnetic Properties of Layered Transition Metals*; de Jongh, L. J., Ed.; Kluwer Academic Pub.: Dordrecht, The Netherlands, 1990; pp 323−78.
(25) Dalal, N. S.; Smirnov, A. I.; Smirnova, T. I.; Belford, R. L.; Katritzky, A. R.; Belyakov, S. A. *J. Phys. Chem. B* **1997**, *101*, 11249−53.
(26) Reinen, D.; Krause, S. *Solid State Commun.* **1979**, *29*, 691−9.

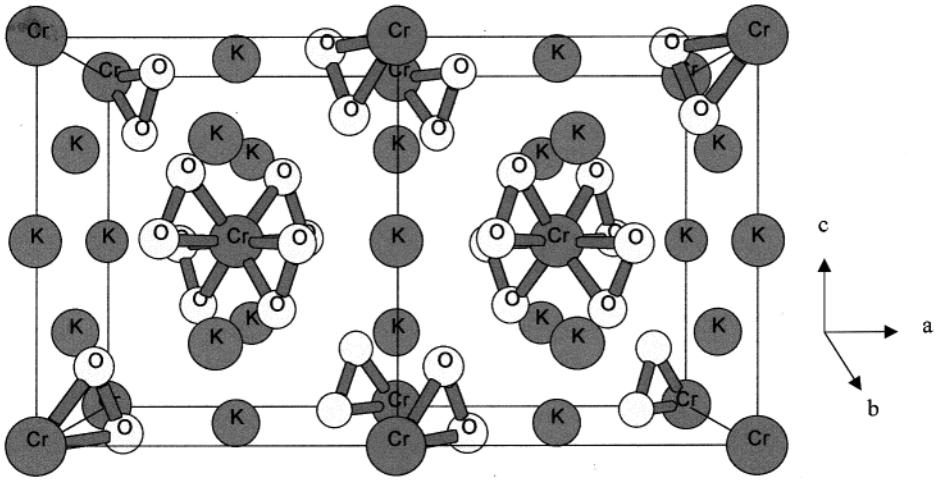

Figure 4. K_3CrO_8 lattice as projected down the *b* axis.

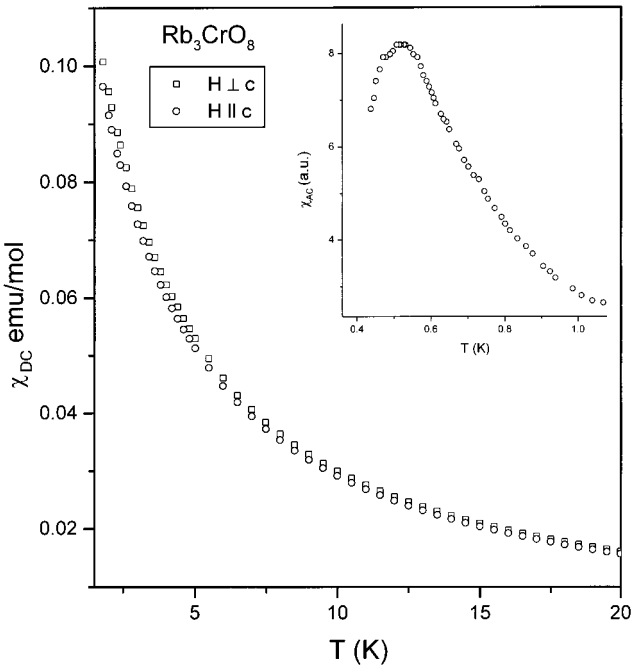

Figure 5. dc magnetic susceptibility of a single crystal of Rb_3CrO_8 with $H \parallel c$ and $H \perp c$ as marked from 1.8 to 20 K. The inset (χ_{ac} (powder) in arbitrary units from 0.4 to 1.2 K) shows the broad peak around 0.52 K.

perpendicular to the applied magnetic field. The inset shows the *ac* susceptibility[9,27] from 0.4 to 1.2 K. A single broad peak is observed with a maximum at 0.52 K. This is to be compared with the T_{max} of 0.82 K for K_3CrO_8. The high-temperature data in Figure 5 have been analyzed using the Curie−Weiss law, $\chi_p = C/(T - \theta)$, using the procedure outlined earlier.[6] The Curie constants (C) and the Curie−Weiss temperatures (θ) are listed in Table 2. The negative values for θ are consistent with dominant antiferromagnetic interactions. Our measurements of the susceptibility down to 0.4 K showed little evidence of three-dimensional long-range ordering, although there is a small anomaly around 0.47 K; however, the data are sparse. Specific heat measurements below 1.8 K are required to determine whether three-dimensional ordering is present.

(27) Kultar, S. Ph.D. Thesis, University of West Virginia, 1986.

III.C.b. Susceptibility and Heat Capacity for the Mixed Cation Lattice K_2NaCrO_8. The magnetic susceptibility of the mixed cation lattice K_2NaCrO_8 was done on a multicrystalline sample, and the data are presented in Figure 6. There is observed a broad maximum at 2.29 ± 0.05 K, a sign of antiferromagnetic low-dimensional behavior. The inset to Figure 6 provides a magnification of the 1.8−5 K region. The drawn and dotted lines are the Bonner−Fisher calculation[14,28] for $N = \infty$ and the quadratic lattice[17,29] (using $g_{ave} = 1.9728$ and J as given in Table 3), respectively. While the shape of the experimental curve is consistent with low-dimensional behavior, the magnitudes of the curves are not; this is under investigation. The constants C and θ are listed in Table 2. The negative value observed for θ indicates that dominant antiferromagnetic interactions are present for this compound as well.

The heat capacity data at a number of magnetic fields (approximately corresponding to integer multiples from 0 to 6 of J/k as determined from susceptibility data) are presented in Figure 7. At $H = 0$ T and 1.8 K one observes what appears to be a high-temperature tail of a λ-type peak, which is then suppressed as the field is increased. This indicates that the peak is of a magnetic origin and possibly representative of the Neel transition. Access to lower temperatures may provide a clearer observation of a three-dimensional ordering or a possible double maximum in C_p vs T at high field.

The field dependence of C_p was compared to that expected for a linear chain[30] and the results are presented in Figure 8. Qualitatively, the 3 K isotherm follows the Bonner−Fisher calculation (drawn line); however, there is some deviation in the magnitude of the minimum at 4 T. These data nevertheless indicate that at $H = 0$ T strong three-dimensional interactions

(28) Hatfield, W. E.; Estes, W. E.; Marsh, W. E.; Pickens, M. W.; ter Haar, W. L.; Weller, R. R. *Extended Linear Chain Compounds*; Miller, J. S., Ed.; Plenum Press: New York, 1983; Vol. 3, pp 43−142.

(29) Numasawa, Y.; Watanabe, T. *J. Phys. Soc. Jpn.* **1976**, *41*, 1903−05.

(30) These calculations are of the variation of the antiferromagnetic Heisenberg case for the mean specific heats for $N = 10$ and 9 (except at $H = 0$ where the estimated limit is given) at integer multiples of $-g\beta H/|J|$ ranging from 0 to 5, as per the 1964 Bonner−Fisher paper. A recent article examines the field dependence of a $S = 1/2$ Heisenberg antiferromagnetic chain; see Hammer, P. R.; Stone, M. B.; Reich, D. H.; Broholm, C.; Gibson, P. J.; Turnbull, M. M.; Landee, C. P.; Oshikawa, M. *Phys Rev. B* **1999**, *59*, 1008−15.

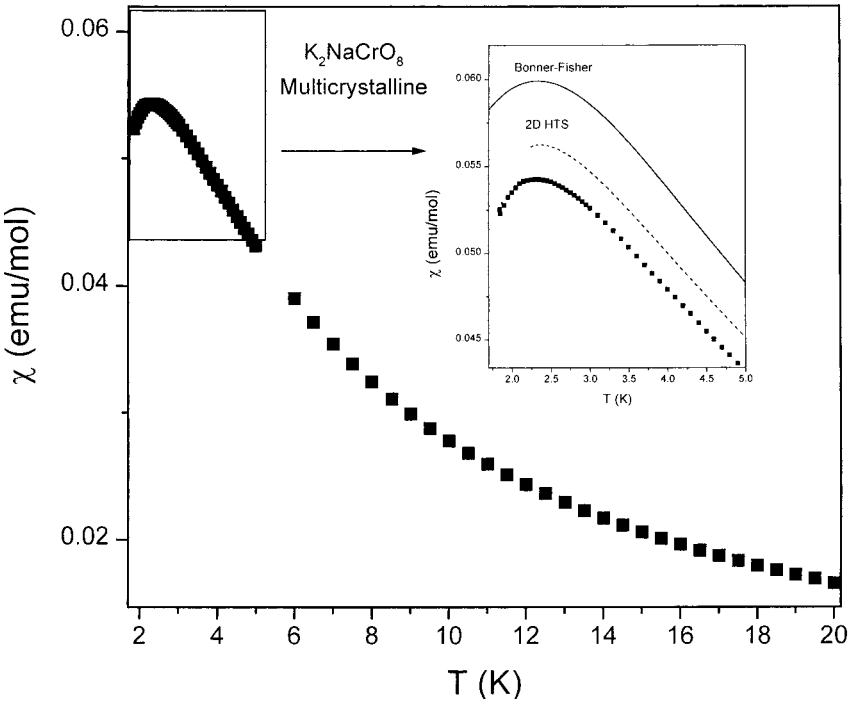

Figure 6. Temperature dependence of χ_{dc} of K_2NaCrO_8 (multicrystalline) from 1.8 to 20 K. Inset magnifies the region between 1.8 and 5 K. The drawn and dashed lines are the Bonner−Fisher $1D_{N=\infty}$ and the 2D HTS as marked.

Table 2. Magnetic Parameters of the Peroxychromates[41] [a]

compound	$\theta_{\|}$ (K)	$\theta_{\perp}$ (K)	$C_{\|}$ (emu·K/mol)	$C_{\perp}$ (emu·K/mol)	b (J·K)/mol
Na_3CrO_8		−5.2	0.368 ± 0.005		
K_2NaCrO_8		−2.3	0.325 ± 0.005		15
K_3CrO_8	−1.6	−1.7	0.353 ± 0.005	0.366 ± 0.005	4.2
Rb_3CrO_8	−1.4	−2.3	0.3341 ± 0.0005	0.3712 ± 0.0005	1.4

[a] Note: The parallel and perpendicular values are given with respect to the crystal c axis; all values for C and θ had a correlation factor of ≥0.9999.

Table 3. Comparison of J/k as Determined by χ and C_p

			exchange energies $-J/k$ (K)					
			$1D_{N=6}$		$1D_{N=\infty}$		2D	
compound	$T_{C_p max}$ (K)	$T\chi_{max}$ (K)	C_p	χ	C_p	χ	C_p	χ
Na_3CrO_8	2.35	3.50	3.11	2.54	2.81	2.73	2.08	1.87
K_2NaCrO_8	<1.8	2.29	1.8	1.66	1.8	1.78		1.22
K_3CrO_8	0.66	0.82	0.76	0.60	0.69	0.64	0.50	0.44
Rb_3CrO_8		0.52		0.38		0.40		0.28

are present, but as the field is increased low-dimensional behavior becomes dominant.

III.C.c. Susceptibility and Heat Capacity for Na_3CrO_8. Figure 9 shows χ_p (where the diamagnetic contribution has been subtracted out) as a function of temperature for Na_3CrO_8. The inset provides χ_p^{-1} over the temperature range of 25−90 K from which C and θ were determined and are listed in Table 2. Again, there is observed a broad maximum at 3.50 K characteristic of short-range interactions. The drawn line provides the Bonner−Fisher infinite chain[14,28] fit and the dashed line provides the two-dimensional lattice fit[17,29] (using g_{ave}=1.9731 and J as given in Table 3). As was the case for K_2NaCrO_8, the shape of the susceptibility is consistent with these fits, but the magnitude of χ_{max} is not, by about the same factor, which is under investigation.

Figure 10 presents C_p as a function of temperature. The main plot is the zero field data, and a broad λ transition is observed with a maximum at 2.35 K, which could well be interpreted as the onset of long-range

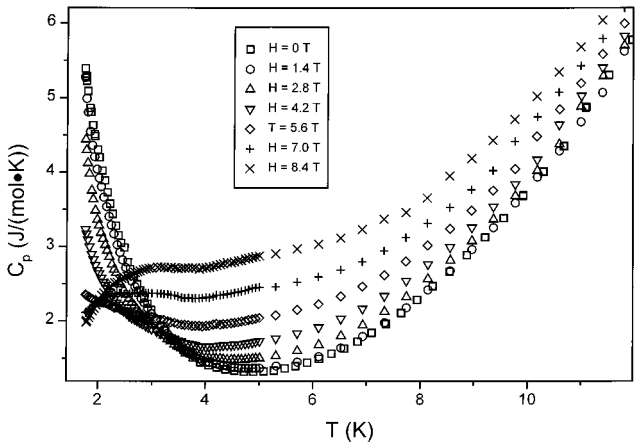

Figure 7. Temperature dependence of the specific heat of K_2NaCrO_8 (multicrystalline) at magnetic fields from H = 0 to H = 8.4 T.

antiferromagnetic order. The specific heat was examined further at magnetic fields of 6 and 9 T (Figure 10 inset). At the magnetic field of 9 T, which is about 4 times the exchange energy of 2.35 K, a temperature shift of ∼0.35 K is observed. Remember, the similar anomaly in the heat capacity of K_2NaCrO_8 (Figure 7) was quite responsive to a field of this magnitude compared to the exchange energy; that is, it was practically extinguished. Other examples in the literature[31] include $MnCl_2·4H_2O$, which possess a classic λ-type peak associated with an antiferromagnetic phase transition in the same tem-

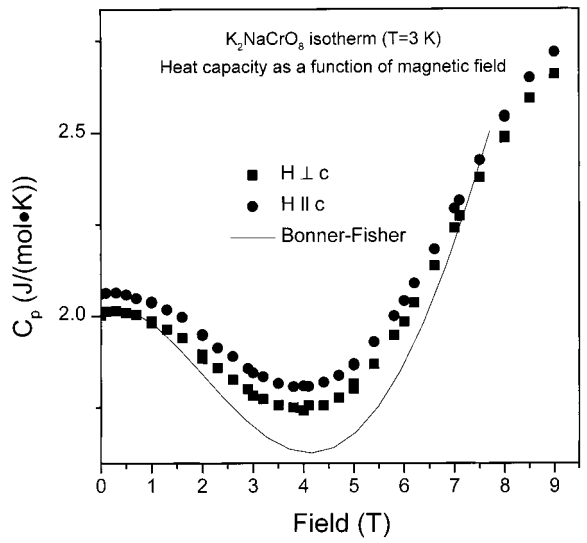

Figure 8. Isothermal specific heat for aligned crystals of K_2NaCrO_8 ($T = 3$ K) with $H \parallel c$ and $H \perp c$ (as marked). Drawn line is the fit for the field dependence of a Heisenberg chain.

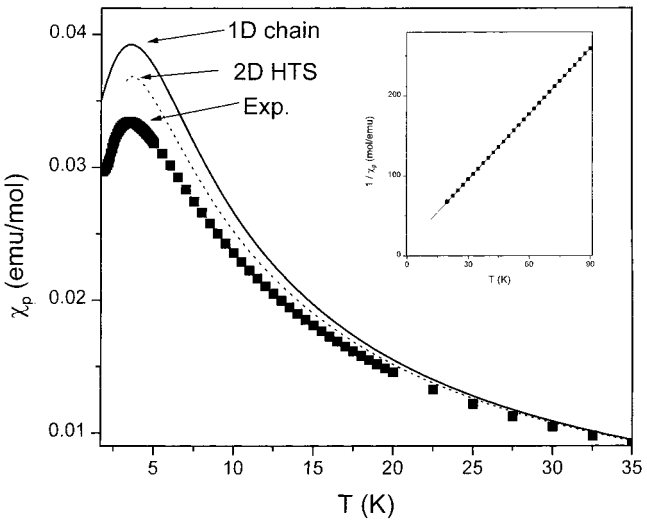

Figure 9. Temperature dependence of χ_p for polycrystalline Na_3CrO_8. Notice the broad peak at 3.50 K. The drawn and dashed lines are fits for a 1D chain and a 2D lattice, respectively. The inset provides $1/\chi_p$, from which C and θ were determined.

perature region, which is entirely suppressed upon application of a 9 T field. Therefore, it is still unclear as to whether the entire transition at 2.35 K is of a magnetic nature. Preliminary EPR studies[32] at fields comparable to the exchange energy down to 1.4 K have revealed data similar to those observed[26] in the lattice distortion of the pyridine-*N*-oxides and are under investigation.

Further analysis of this transition is given in Figure 11, which presents the acquisition of magnetic entropy as a function of temperature at $H = 0$ T. As shown in section III.A.b, the expected total possible magnetic contribution to the entropy is 5.76 J/(mol·K), which is approached asymptotically. If one calls the transition at 2.35 K the antiferromagnetic ordering temperature, or T_N, then it is observed that >60% of the magnetic

(31) Reichert, T. A.; Giaque, W. F. *J. Chem. Phys.* **1969**, *50*, 4205–22.

(32) Cage, B.; Brunel, L.-C.; Dalal, N. S. unpublished results.

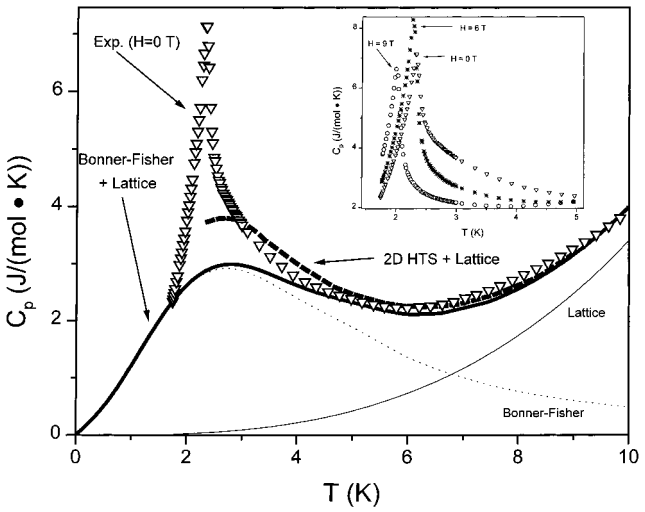

Figure 10. Specific heat of polycrystalline Na_3CrO_8 as a function of temperature. Main plot is the $H = 0$ T data. The underlying low-dimensional magnetic behavior is fit by use of the sum (solid line) of the Bonner–Fisher calculation,[14] where $N = \infty$ (dotted line), and the lattice term (as marked). Also, the fit for the 2D HTS + lattice is given as the dashed line. Inset provides the field dependence of the λ transition at $H =$ 0 (▽), 6 (*), and 9 (○) T.

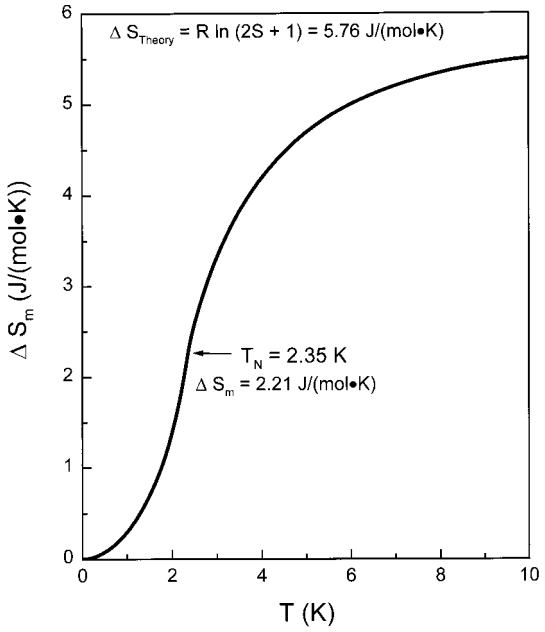

Figure 11. Magnetic entropy acquisition of Na_3CrO_8 as a function of temperature (extrapolated below 1.8 K) at $H = 0$ T. This plot shows that over 60% of the magnetic entropy is involved in short-range interactions above T_N (as marked).

entropy is involved in short-range interactions above T_N. Therefore, even if all or only a portion of the peak at 2.35 K is associated with the onset of long-range order, a majority of the spin entropy is engaged in short-range activity above 2.35 K and thus requires accounting.

The data in Figure 10 were therefore fit by use of the sum (solid line) of the Bonner–Fisher calculation,[14] where $N = \infty$ (dotted line) and the lattice term (as marked), which was a free fitting parameter using the Debye cube law. Also, the fit for the two-dimensional HTS + lattice is given[16–18] (dashed line). The exchange energies for both fits as determined from C_p are compared to those from χ in Table 3, and reasonable

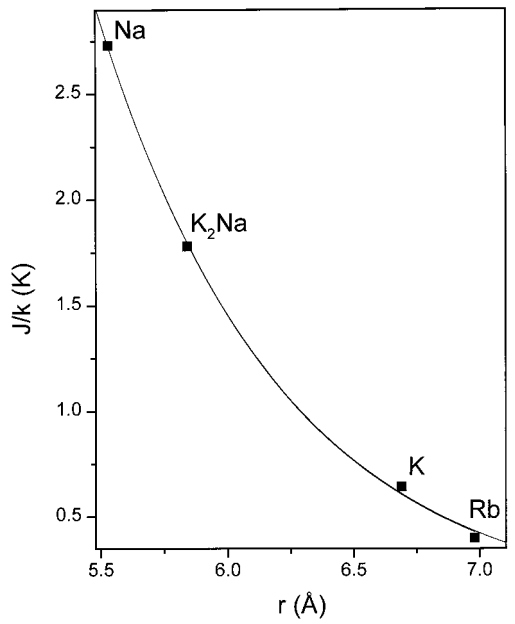

Figure 12. Plot of the exchange energy as determined from Bonner−Fisher analysis of χ vs Cr−Cr distance (r). Drawn line is an empirical fit using an exponential decrease as a function[43] of r. This plot may find use as a predictive tool for the optimum ionic distances required for tuning the peroxychromates as heat sinks and magnetic refrigerants at a desired temperature.

agreement is present for both. The fit to the two-dimensional lattice in both Figures 9 and 10 appears to be somewhat better than the Bonner−Fisher chain, and perhaps EPR measurements may help distinguish between the two. Nonetheless, this agreement between C_p and χ, coupled with the fact that a majority of entropy is acquired above T_N (Figure 11), provides strong evidence that low-dimensional spin interactions are predominant for this compound as well.

III.D. Cation Effects on Susceptibility Peak Temperatures. To understand the mechanism underlying the magnetism of these compounds, we examined the relationship of J/k as obtained from χ (Table 3, $1D_{N=\infty}$) to the Cr(V) interion distance (r). A plot of $|J|/k$ vs r is shown in Figure 12. Clearly, J seems to have an exponential dependence on the ionic distance (drawn line). The data in Figure 12 are qualitatively rationalized on the basis of the well-established fact that should the exchange mechanism be kept the same, then an increase in interion distance results in a decrease of the exchange energy,[33] which implies a decrease in $T\chi_{max}$ (temperature at which χ is maximum). These data indicate that a simple relationship exists whereby $T\chi_{max}$ of the peroxychromates may be manipulated over a wide temperature range by variation of the counterions of the peroxychromates. Figure 12 allows for the estimation of the temperature at which C_p is maximized (T_{C_pmax}) as a function of the ionic distance (since[14,19] $T\chi_{max}/T_{C_pmax} \sim 1.3$). Therefore, a promising area of research is dilution with a diamagnetic host such as K_3NbO_8 or molecular substitution to manipulate ionic distance and tune T_{C_pmax} to a desired temperature. The value of this finding is the potential to tune the peroxychromates as heat sinks and magnetic refrigerants throughout the mK to 5 K temperature range, as will be discussed in section IV.

III.E. EPR Determination of the Electronic Ground State. The ground state of the lone $3d^1$ electron of the CrO_8^{3-} ion can be easily determined using EPR spectroscopy.[6,34] The hybridization[6] of the peroxychromates has been shown to be d^4sp^3 with the unpaired electron residing in either the d_{z^2} orbital or the $d_{x^2-y^2}$ orbital. A tetragonal distortion of the crystal field removes the degeneracy. For a tetrahedron a compression[35] along z, the high-symmetry axis, makes the d_{z^2} orbital lie lowest in energy. However, an elongation along z results in the $d_{x^2-y^2}$ orbital being lowered in energy.

In the case of a compressed tetrahedron the g factors are[35] $g_z = g_{||} = g_e$ and $g_\perp = g_e - 6\lambda/\Delta E_{xz}$, where $g_{||}$ and $g_\perp$ are the parallel and perpendicular[36] g factors, g_e is the free electron g value (2.0023), λ is the spin−orbit coupling constant, and ΔE_{xz} is the energy separation between the d_{z^2} and d_{xy} orbitals.[37] These relationships imply that, in the case of a d_{z^2} ground state for a $3d^1$ ion, $g_\perp < g_{||}$.

For an elongated tetrahedron the g factors are $g_z = g_{||} = g_e - 8\lambda/\Delta E_{xy}$ and $g_\perp = g_e - 2\lambda/\Delta E_{xz}$ where ΔE_{xy} and ΔE_{xz} are the energy separations between the $d_{x^2-y^2}$ and the d_{xy} and d_{xz} levels, respectively. These relationships imply that in the case of a $d_{x^2-y^2}$ ground state for a $3d^1$ ion, $g_\perp > g_{||}$.

As a typical example, the EPR spectrum of Rb_3CrO_8 powder at two frequencies is presented in Figure 13. The spectra result from the Zeeman interaction of the $3d^1$ unpaired electron on the $^{50,52,54}Cr$ (90.5% natural abundance) isotopes. Thus, to a good approximation there is no hyperfine interaction expected, and the spectra should reflect peaks at the principal values of the **g** tensor for each compound. For a lattice with tetragonal symmetry, we thus expect the spectra to exhibit only two peaks in the first-derivative presentation: one corresponding to the resonance absorption of molecules whose tetragonal axis is oriented along the Zeeman field (labeled $g_{||}$), and the other absorption from those molecules whose tetragonal axis is aligned perpendicular to the field direction (labeled $g_\perp$). The inset is at the X-band frequency ($\nu \sim 9.5$ GHz), and the peaks are labeled $g_\perp$ and $g_{||}$. At higher frequency ($\nu \sim 95$ GHz) there is an order of magnitude better resolution of the spectrum and it is easily determined that $g_\perp > g_{||}$ (see Table 4); the ground state is then $d_{x^2-y^2}$.

III.F. Change of the Electronic Ground State in Mixed Crystals. A surprising result was that substitution of Na^+ ions into monocationic lattices forming "mixed crystals" (i.e., K_3CrO_8 to K_2NaCrO_8 and Rb_3CrO_8

(33) De Jongh; L. J.; Block, R. *Physica* **1975**, *79B*, 568−93.

(34) McGarvey, B. R. *Electron Spin Resonance of Metal Complexes*; T. F. Yen, Ed.; Plenum Press: New York, 1969; pp 1−11.

(35) Weil, J. A.; Bolton J. R.; Wertz, J. E. *Electron Paramagnetic Resonance*, 2nd ed.; Wiley and Sons: New York, 1994; pp 221−27.

(36) In the case of a tetragonal system $g_\perp$ is composed of the degenerate g_x and g_y factors. These may be resolved in lower symmetry lattices in which case $g_{||}$ is referred to as g_z.

(37) The parallel g value can deviate from the free electron value due to small distortions from axial symmetry, which results in a small admixture of the $d_{x^2-y^2}$ orbital. It is noted that these relationships are based on a purely ionic model and must be slightly modified due to covalent bonding; however, the general relationships are not changed by these small deviations.

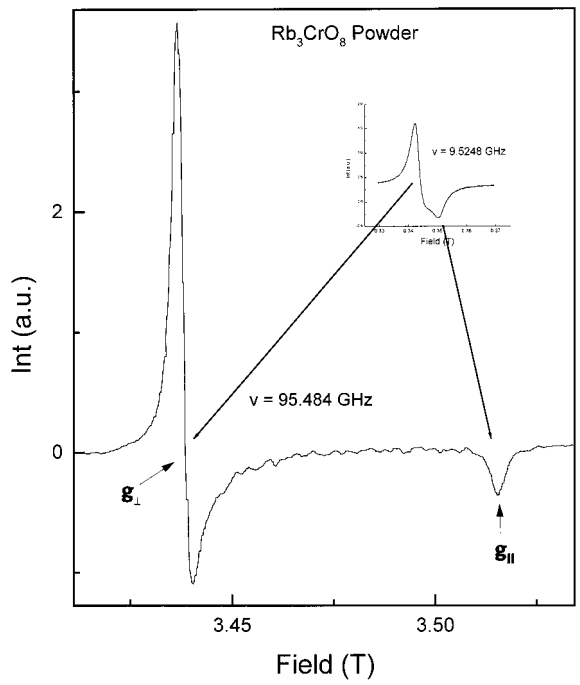

Figure 13. EPR spectra of Rb_3CrO_8. The inset is at the *X* band, ~9.5 GHz, a 10-fold increase of the microwave frequency to 95 GHz (lower plot) provides superior resolution of the **g** tensor, and it is determined $g_\perp > g_{||}$, and therefore the electronic ground state is $d_{x^2-y^2}$.

Table 4. *g* Values and Electronic Ground States of the Unhydrated Peroxychromates[42]

compound	g_z (±0.0005)	g_y (±0.0005)	g_x (±0.0005)	electronic ground state
Na_3CrO_8	1.9544	1.9802	1.9848	$d_{x^2-y^2}$
K_3CrO_8	1.9431	1.9852		$d_{x^2-y^2}$
K_2NaCrO_8	1.9851	1.9696	1.9636	d_{z^2}
Rb_3CrO_8	1.9426	1.9825		$d_{x^2-y^2}$
Rb_2NaCrO_8	1.9849	1.9688	1.9633	d_{z^2}

to Rb_2NaCrO_8) changed the electronic ground state. As an example, the EPR spectrum of Rb_2NaCrO_8 is presented in Figure 14. The inset is at the *X* band (9.15 GHz) and due to lack of peak resolution at this low frequency the details of the ground state cannot be ascertained. On the other hand, the 95-GHz spectrum is unambiguous and it is found that $g_z > g_y > g_x$, where g_z is the parallel value and g_y and g_x are the two perpendicular values of the *g* tensor, respectively. These results show that exchange of Na for just one Rb has changed the electronic ground state from $d_{x^2-y^2}$ to d_{z^2} (compare Figures 13 and 14). Further, the appearance of three peaks for Rb_2NaCrO_8 indicates that the tetragonal symmetry of the system has been lowered. Similar results have been obtained for all the M_3CrO_8 lattices. Table 4 provides the room-temperature *g* values, as obtained at the *W* band, for various cation combinations of the peroxychromates, from which the electronic ground states were determined.

The calculated electronic ground state of the unpaired electron for K_3CrO_8 has been shown by numerous researchers[7a,b,38] to be $d_{x^2-y^2}$, in agreement with experimental results.[6] With a view to understanding the

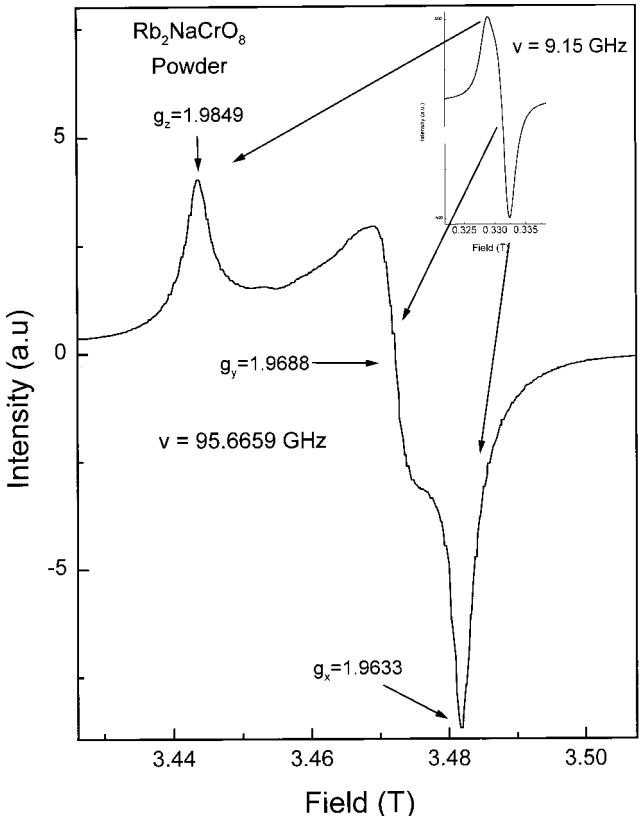

Figure 14. EPR spectra Rb_2NaCrO_8. The *X*-band spectrum, ~9.1 GHz (inset), is poorly resolved; however, the 95 GHz spectrum (lower) provides an unambiguous determination of the **g** tensor such that $g_z > g_y > g_x$. This proves the exchange of one Na for one Rb ion has dramatically changed the electronic ground state from $d_{x^2-y^2}$ to d_{z^2} (compare with Figure 13). Similar results were observed for K_2NaCrO_8.

difference in the electronic ground state of K_2NaCrO_8 from the K_3CrO_8 and Na_3CrO_8 salts, we examined the crystal structure of K_2NaCrO_8.[10] Figure15 presents the K_2NaCrO_8 lattice projected down the *b* axis, and the parameters are listed in Table 1. EPR allowed the determination of the magnetic *z* axis (g_{zz}) with respect to the crystal morphology. By use then of Appendix A, we found that g_{zz} corresponds to (0,0,1) for K_3CrO_8 and (1,1,0) for K_2NaCrO_8. Table 5 presents the bond lengths and angles of the labeled atoms in Figure 1 for the three salts.

The CrO_8^{3-} dodecahedral structure in Figure 1 may be thought of as built from two interlocking distorted tetrahedra. One, a compressed tetrahedron essentially in the *xy* plane (of which O_b and $O_{b'}$ are two mirror symmetry-related atoms) and the other extended along the *z* axis (of which O_a and $O_{a'}$ are two mirror symmetry-related atoms). It appears that the latter is the dominating factor, rendering $d_{x^2-y^2}$ as the electronic ground state for all of the M_3CrO_8 salts, with M = Na, K, Rb, in agreement with theoretical calculations.[7,38] For the case of the mixed salt, K_2NaCrO_8, the anion geometry is not radically different as compared to those of the pure Na and K salts, and it is difficult to explain the origin of the experimentally observed d_{z^2} ground state on the basis of the data in Table 5. Similar results have been observed for Cr(V) doped in YVO_4 and YPO_4, which were attributed[39] to the influence of the second coordination sphere. Therefore, other factors such as the

(38) Cundari, R. T.; Zerner, M. C.; Drago, R. S. *Inorg. Chem.* **1988**, *27*, 4239−41.

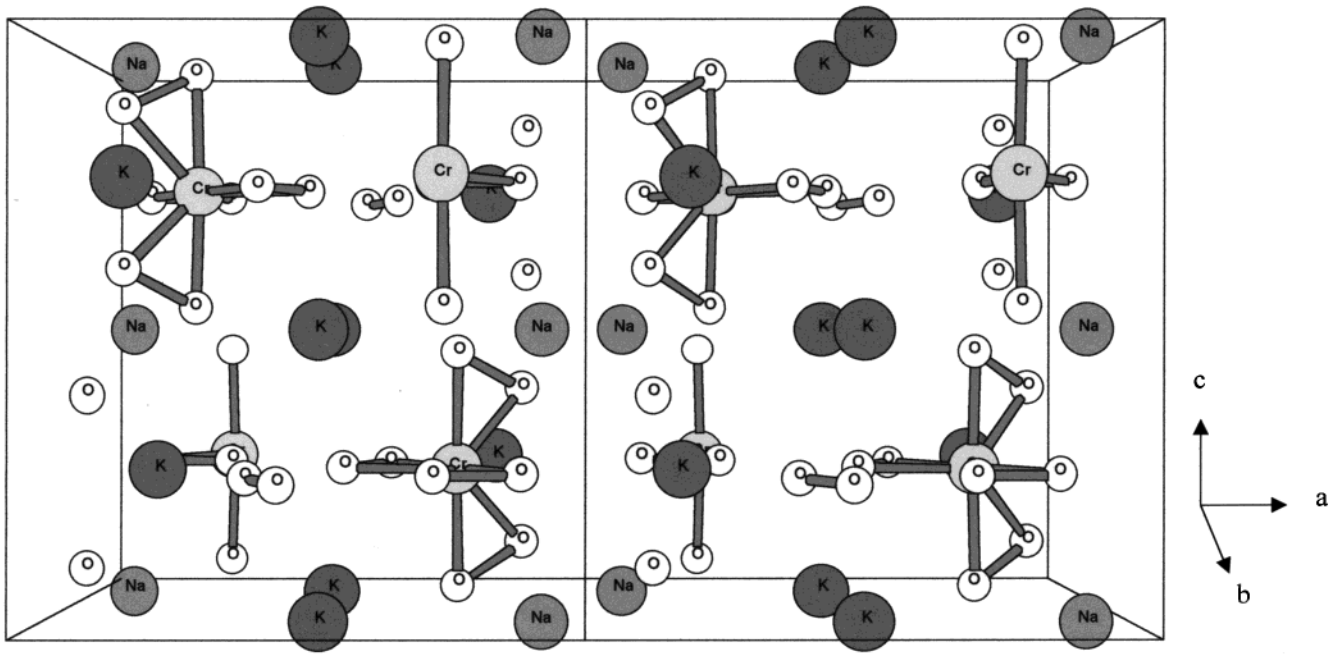

Figure 15. K_2NaCrO_8 lattice as projected down the *b* axis.

Table 5. Comparison of Some Bond Lengths (Å) and Angles (°)[10]

compound	Cr−O_a	Cr−O_b	O_a-Cr−$O_{a'}$	O_b-Cr−$O_{b'}$	g_{zz}
K_3CrO_8	1.8812	1.9584	85.46	174.21	(0,0,1)
K_2NaCrO_8	1.8896	1.9463	88.7	177.05	(1,1,0)
Na_3CrO_8	1.893	1.9313	88.75	177.61	

distribution of the cations throughout the lattice must be coming into play, and detailed theoretical calculations are required to understand this ground-state inversion for the mixed salts K_2NaCrO_8 and Rb_2NaCrO_8.

IV. Utility as Heat Sinks and Magnetic Refrigerants

Due to the cationic temperature dependence of the large specific heats in the mK to 4 K region, a possible utilization of the peroxychromates may be as tunable heat sinks. Table 3 provides the temperatures at which C_p is at maximum (where available). These data indicate the temperature regions of greatest utility; that is, K_3CrO_8 or Rb_3CrO_8 would be ideal as heat sinks between 0.3 and 1.5 K while Na_3CrO_8 would be useful in the 1.5−5 K range. Further work has indicated that the hydrated peroxychromates are valuable as heat sinks in the <0.3 K region, as is discussed in a related paper.[23]

Analysis of heat capacity data suggests that a solid solution of K_3CrO_8 in the diamagnetic matrix K_3NbO_8 may be a good candidate as a tunable magnetic refrigerant. This claim is supported by the heat capacity coefficient (*b*), which is derived from the high-temperature behavior of the magnetic specific heat such that $C_m = b/T^2$. The lower the magnitude of *b*, the greater the magnetic refrigerant potential,[19] and the lower the minimum operating temperature. The data in Tables 1 and 2 indicate that small increases in the Cr−Cr distance significantly lowers the value of *b*. Notable is that the 50% solid solution of K_3CrO_8/K_3NbO_8 is calculated[40] to have an order of magnitude lower value of *b* and about twice the spin concentration of the magnetic refrigerant $Ce_2Mg_3(NO_3)_{12}\cdot 24H_2O$ (CMN). This implies it should be superior to CMN in the important <100 mK region. Further, since *b* is obtained from the high-temperature tail[19,40] of C_m, and C_m can be estimated[40] from J/k, then Figure 12 may find use as a predictive tool for the optimum bond distances required for tuning the peroxychromates as magnetic refrigerants and heat sinks (where[14,19] $kT_{C_p max}/|J| \sim 0.96$) at a desired temperature.

V. Conclusion

The above-presented magnetic susceptibility, EPR, and specific heat data show for the first time that the Cr(V) peroxychromates possess a wide variety of valuable magnetic properties; these include large specific heats in the range of mK to 5 K, low-dimensional spin behavior, and antiferromagnetic spin ordering. In particular, the agreement of exchange energies as determined by C_p and χ fits indicates that the magnetic behavior is of a low-dimensional nature. These characteristics coupled with their simple electronic structure render the peroxychromates valuable as theoretical models for metal-oxide spin exchange calculations. The physical properties have been shown to be convenient for experimental work: these include stability over a wide temperature range, that is, mK to 373 K, insen-

(39) Hazenkamp, M. F.; Stuckl, A. C.; Cavalli, E.; Gudel, H. U. *Inorg. Chem.* **2000**, *39*, 251−4.

(40) Cage, B.; Dalal, N. S. *J. Appl. Phys.* **2000**, *87* (9), 6031−33.

(41) Earlier work has been done on powder samples in refs 6 and 27.

(42) Earlier work at the *X* band has been done in refs 6, 7a, and 27. Earlier high-field EPR work can be found in Cage, B.; Hassan, A. K.; Pardi, L. Krzystek, J.; Brunel, L.-C.; Dalal, N. S. *J. Magn. Reson.* **1997**, *124*, 495−8.

(43) The explicit function is $|J|/k = 0.076$ K + (2.65 exp(−(r − 5.53 Å)/0.72 Å)) K where r is the Cr−Cr distance along the preferred exchange axis $|J|/k$ is the exchange energy in Kelvin.

sitivity to air and light, large single crystals that are easily grown, simple crystal structures, and the relationship of the magnetic symmetry axis to the crystal morphology can easily be determined by EPR. Also, this work has shown that the exchange energies are of the same order as the magnetic fields currently being explored in state of the art high-field EPR (1−16 T) and may find interest from that standpoint. These compounds are predicted to find useful applications as heat sinks and magnetic refrigerants in the mK to 5 K region.

We reiterate that some issues remain unresolved. First, it has not been possible to provide an explanation for the electronic ground-state inversion of the mixed salts, K_2NaCrO_8 and Rb_2NaCrO_8, given that the geometry of the CrO_8^{3-} anion is not dissimilar to that of the pure salts of K and Na. Second, it is not clear from crystal structures obtained at ~173 K why these compounds should exhibit low-dimensional spin exchange behavior, and from the data herein as to the exact lattice dimensions, that is, one-dimensional (1D) or two-dimensional. Further work involving local measurements such as EPR or NMR are required to precisely define the nature of the exchange interactions. Theoretical calculations and structural studies using X-ray and/or neutron techniques at liquid helium temperatures should also be quite fruitful.

Acknowledgment. This work was initiated when N.S.D was at West Virginia University. He wishes to thank Drs. K. A. Abboud, K. Singh, J. S. Moodera, B. Craven, and S. Friedman for help with initial studies as summarized in refs 9 and 10. In addition, B.C. would like to thank Dr. S. McCall of FSU/NHMFL for some helpful assistance with experimental work and K. Collins of FSU chemistry for technical assistance with the assembly of the 95 GHz EPR probe. We wish to thank the National Science Foundation for partial support of this work.

Appendix A

Relation of the crystal morphology to the crystal axes for the nonhydrated peroxychromates:[10,27]

CM000643D

K_3CrO_8, Rb_3CrO_8

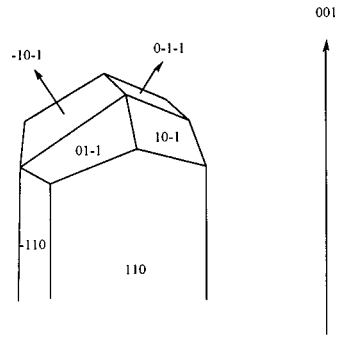

Na_3CrO_8

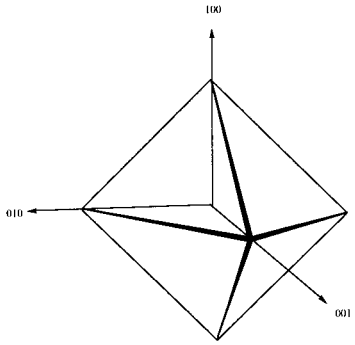

K_2NaCrO_8